Reconfigurable coupled-resonator acoustoelastic waveguides in fluid-filled phononic metaplates

Ting-Ting Wang[a], Yan-Feng Wang[b,1], Zi-Chen Deng[a], Vincent Laude[c,2], Yue-Sheng Wang[b,d]

[a]*School of Mechanics, Civil Engineering and Architecture, Northwestern Polytechnical University, 710072 Xi'an, China*
[b]*School of Mechanical Engineering, Tianjin University, 300350 Tianjin, China*
[c]*Institut FEMTO-ST, Université de Bourgogne Franche-Comté, CNRS, 25030 Besançon, France*
[d]*Institute of Engineering Mechanics, Beijing Jiaotong University, 100044 Beijing, China*

Abstract

We study numerically and experimentally acoustoelastic wave propagation in a two-dimensional phononic metaplate consisting of a periodic array of cups sitting on a thin epoxy plate that is perforated with cross holes. When all cups are filled with water, the metaplate possesses a complete band gap. Reconfigurable coupled-resonator acoustoelastic waveguides (CRAEWs) are created by locally emptying certain cups, thus introducing local resonances that are evanescently coupled. Straight and 90° bent periodic waveguides are considered, together with an aperiodic chain of 11 coupled resonators. The aperiodic chain has no definite spatial periodicity but supports collective resonances resulting from the coupling of nearest resonators. Lamb waves are experimentally excited by a piezoelectric patch and received by a scanning optical vibrometer. Experimental results for acoustoelastic wave propagation along both periodic and aperiodic CRAEWs are compared to a three-dimensional finite element model taking fluid-structure interaction into account. The propagation of confined acoustoelastic waves in the 90° bent waveguides and the collective resonances of the aperiodic chain of defected resonators are observed experimentally. Reconfigurability are realized based on the coupling of acoustoelastic waves in a phononic metaplate. Our results show plenty of potential possibilities for the practical design of reconfigurable and programmable elastic wave devices.

Keywords: Phononic crystal, Reconfigurable waveguide, Coupled-resonator acoustoelastic waveguides

1. Introduction

Phononic crystal (PC) is a new type of periodic functional composite material [1, 2] possessing frequency band gaps within which the propagation of acoustic/elastic waves is completely forbidden [3]. Stated otherwise, Bloch waves become evanescent inside band gaps [4]. A coupling mechanism for the vibrations of chains of masses connected by springs [5, 6] or of coupled-resonator waveguides [7] is provided by those evanescent waves. Furthermore, strong localization of waves in the phononic band gap can be achieved. [8, 9, 10]. When the periodicity of a perfect phononic crystal is destroyed locally, defect states appear. Waves within the band gap are confined into the defects [11] and decay rapidly far away from them. The guidance of acoustic or elastic waves can thus be realized by designing defects in a perfect phononic crystal. The introduction of defects provides new ideas to manipulate waves, and to design and manufacture novel acoustic devices with phononic crystals, and has attracted widespread attention. Linear lines of defects [12, 13, 14], as the most commonly used guidance mechanism, are thus formed to channel waves at selected frequencies in the band gap with strong confinement [15, 16], promising a variety of potential applications [17, 18] such as sensing [19, 20, 21, 22, 23, 24], filtering [25], or waveguiding [14, 26, 27].

The concept of the coupled-resonator optical waveguide (CROW) defined in a photonic crystal [28, 29] has been extended in recent years to the field of phononic crystals. Overall, the propagation of waves in evanescently coupled waveguides stands as simple and efficient among the various physical mechanisms for guiding waves in artificial crystals. In contrast to linear-defect waveguides, the coupled-resonator waveguide is based on the evanescent coupling of defect cavities or

[1]corresponding author. E-mail address: wangyanfeng@tju.edu.cn
[2]corresponding author. E-mail address: vincent.laude@femto-st.fr

resonators [5, 6], permitting the design of rather arbitrary acoustic circuits [30, 31]. The coupling between neighboring defect cavities or resonators creates a propagating dispersion band with a small slope (slow sound) appearing around the flat band generated by the isolated point defect. If the frequency of the defect state is inside a complete band gap of the perfect structure, the defect state is completely localized. The field beyond the defect is evanescent, decaying exponentially away from the defect. Waveguides based on linear chains of coupled cavities have been shown theoretically to allow simultaneously for very strong wave confinement [8, 9, 10] and for low group velocity transmission [31]. It is conducive to design new and efficient acoustic devices. In fact, as long as the distance between resonators remains limited and the resonance frequencies are the same, any defect chain of defect cavities or resonators can form a waveguide [32]. This is the basic idea of a coupled-resonator waveguide. Coupled-resonator waveguides do not only manipulate wave propagation by changing the length of the waveguides [33], they also regulate the dispersion relation by changing the distance between adjacent resonators [34], the number of resonators along the circuit, or the coupling coefficient between resonators.

To date, some works have focused experimentally on elastic or acoustic wave guiding along coupled-resonator waveguides. Mohammadi et al. realized an effective band-pass filter for wireless communication based on a coupled-resonator acoustic waveguide (CRAW) designed in a phononic crystal plate [35]. Wang et al. investigated coupled resonator elastic waveguides designed in a PC slab with cross holes [26]. The transmission of strongly confined Lamb waves along a straight waveguide and in a wave splitter circuit with 90° bends were observed experimentally. However, the conventionally designed and fabricated structures can hardly have tunable (or reconfigurable) topologies or material parameters, limiting the manipulation of waves.

Many researchers have devoted a lot of efforts to the design, development, and demonstration of tunable PCs and metamaterials resulting in an emerging revolution for tunable, active, or even smart control of acoustic or elastic waves. Tunable or active ways of manipulating waves either based on multifield coupling effects [36, 37, 38] or by mechanical means [26, 39] are investigated. Li et al. tuned the propagation direction of the flexural wave by active control system behaved as the piezoelectric patches on a plate with T-shaped waveguide [40]. Pennec et al. confined and guided sound and light waves with certain frequencies in the associated band gaps by engineering the point and linear defects [41]. Hu et al. investigated the temperature effects on the defect states by changing the temperature of the central rod of the two-dimensional ferroelectric ceramic plate and realize the manipulation of elastic waves in the band gaps [42]. Mazzotti et al. investigated the effect of a generic state of prestress on the passbands and bandgaps of a phononic crystal plate [43].

Among the means for tunable or active manipulation of waves, fluid-solid coupling is a rather easy way to realize reconfigurability for a phononic crystal [44, 45]. Fluid-solid coupling is also suitable to achieve active and smart control of acoustic/elastic waves. How to realize reconfigurability of coupled resonator waveguides is still an urgent problem to be solved. In general, almost all works tackling this problem are limited to numerical simulations and a small amount of theoretical analysis, and lack experimental verification. In previous researches, some unnecessary limitations to the periodic array of resonator chains were set on the design of coupled resonator waveguides [30, 31]. However, evanescent coupling of waves across a band gap is omnidirectional, decreasing exponentially away from a resonator. Therefore, evanescent waves suitably couple adjacent resonators placed along a rather arbitrary path, forming an aperiodic coupled-resonator chain [46].

In this paper, we aim at investigating two-dimensional phononic metaplates consisting of a periodic array of cups sitting on a thin epoxy plate that is perforated with periodic cross holes [47, 48]. When all cups are filled with water, the metaplate possesses a complete band gap. Reconfigurable coupled-resonator acoustoelastic waveguides (CRAEWs) are created by locally emptying certain cups, thus introducing local resonances that are evanescently coupled. We first discuss the dispersion relation of the bare phononic crystal. Then, different waveguides are designed by emptying selected cups. An aperiodic negative chain with 11 coupled resonators is formed respecting an equal-coupling scheme. 3D finite element computations accounting for fluid-structure interaction are compared with experimental measurements. In general, Numerical and experimental results are found to be in good agreement with a slight resonance frequency shifts. Strong acoustoelastic waves confinement is effectively observed in all cases.

2. Methods

In this work, the unit cell of the metaplate consists of a single cup grafted onto a plate with periodic cross holes, as shown in Figure 1(a). Following Ref. [45], geometrical parameters of the unit cell are

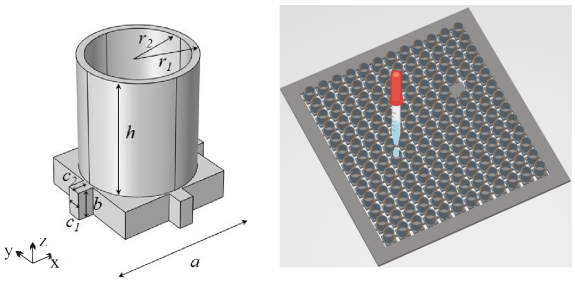

Figure 1: (a) Schematic of the PC unit cell and definition of geometrical dimensions. (b) A finite 3D-printed epoxy metaplate sample consisting of 13 × 12 periodic unit cells. One cup is removed inside the phononic structure to bond a piezoelectric patch for excitation of Lamb waves. Each cup can be individually filled with water. Coupled-resonator acoustoelastic waveguides are thus defined in a reconfigurable and re-usable manner. Imaging of wave propagation is performed on the bottom side of the metaplate.

a=5 cm, h=0.8a, b=0.2a, c_1=0.1a, r_1=0.38a, r_2=0.33a, and c_2=0.11a. With this set of parameters, certainly wide band gap is obtained. The epoxy metaplate sample shown in Fig. 1(b) is processed by 3D printing technique.

Wave propagation is measured at the bottom surface of the epoxy metaplate by Polytec PSV-500 scanning vibrometer, associating with the periodic chirp as the source waveform. Then the vertical displacement vibration is formed by a vertically polarized piezoelectric patch bonded to the sample. Experimental transmissions and displacement distributions are finally integrated by detecting and averaging the vertical displacements around the scan points at the bottom side of the sample.

To evaluate numerically the transmission properties of the considered systems, the 3D finite element method is used. Phononic band structures are obtained by solving an eigenvalue problem [31]. Based on Bloch's theorem, two-dimensional Bloch-Floquet periodic boundary conditions are applied on pairs of opposite boundaries of the unit cell depicted in Fig. 1(a) with free bottom and top surfaces. After the finite mesh of the unit cell is created adaptively, it is divided into finite elements connected by nodes. At the interface between fluid and solid, a fluid-solid boundary condition relating the pressure in the fluid to the normal displacement of the solid boundary is imposed. For the filled cup, a sound-soft boundary condition is applied on the top surface of the liquid column. Considering fluid-solid interaction, the discrete form of the acousto-elastic equations is [49]

$$\begin{pmatrix} \mathbf{K}_s & \mathbf{S}_{fs}^T \\ \mathbf{0} & \mathbf{K}_f \end{pmatrix} \begin{pmatrix} \mathbf{u} \\ p \end{pmatrix} - \omega^2 \begin{pmatrix} \mathbf{M}_s & \mathbf{0} \\ -\mathbf{S}_{fs} & \mathbf{M}_f \end{pmatrix} \begin{pmatrix} \mathbf{u} \\ p \end{pmatrix} = \begin{pmatrix} \mathbf{F} \\ 0 \end{pmatrix}, \quad (1)$$

where $\mathbf{u}$ and p represent the displacements and the pressure at the nodes of the solid and fluid field mesh, respectively. $\mathbf{F}$ are nodal forces. $\mathbf{K}_s$ and $\mathbf{K}_f$ are the stiffness matrices of the solid and fluid; $\mathbf{M}_s$ and $\mathbf{M}_f$ are the mass matrices of the solid and fluid; $\mathbf{S}_{fs}$ represents the fluid-solid coupling matrix and $\mathbf{S}_{fs}^T$ is its transpose.

Bloch's theorem is applied on the boundaries of the unit cell in the direction where periodicity applies, yielding the following relation between displacements at the nodes on the boundary of the unit cell:

$$\mathbf{u}(\mathbf{r} + \mathbf{a}) = e^{i\mathbf{k}\cdot\mathbf{a}}\mathbf{u}(\mathbf{r}), \quad (2)$$

where $\mathbf{r}$ is located at the boundary nodes and $\mathbf{a}$ is the lattice constant vector. We solve directly the eigenvalue problem Eq. (1) given the wavevector $\mathbf{k}$ under the complex boundary condition Eq. (2). We thus get the whole band structure when the wavevector $\mathbf{k}$ sweep the irreducible Brillouin zone. According to the dynamic equilibrium Eq. (1), we obtain both the pressure field in the fluid and the displacements field in the solid.

Then the frequency response is estimated as follows. Since a finite phononic crystal and an external source of waves are considered, the finite computational domain has to be terminated with radiation boundary conditions to minimized unwanted reflections. For simulation, a time harmonic and spatially random wave source of vertical polarization is used at the source region where a cup is removed to allow a direct comparison with experiments [50]. By sweeping the excitation frequency f, we evaluate the frequency response function (FRF) $R(f)$ in decibels units by considering the ratio of the z-component of the displacements integrated over the source and the receiver as

$$R(f) = 20\log_{10}\left(\frac{\int_{S_r} u_z \mathrm{d}s}{\int_{S_s} u_z \mathrm{d}s}\right). \quad (3)$$

where u_z is the vertical displacement along S_r, the area of the receiver and S_s, the area of the source.

In this work, the solid material parameters for epoxy are mass density ρ_s = 1175 kg/m^3, Poisson's ratio υ = 0.41, and Young's modulus E = 3.2 GPa. The fluid material is water with mass density ρ_f = 1000 kg/m^3 and sound velocity c = 1490 m/s. Here, the influence on transmission of the viscosity of water and the viscoelasticity of epoxy which are the main sources of damping is neglected for large lattice constants and low frequencies [34].

We first consider the perfect PC metaplate for later

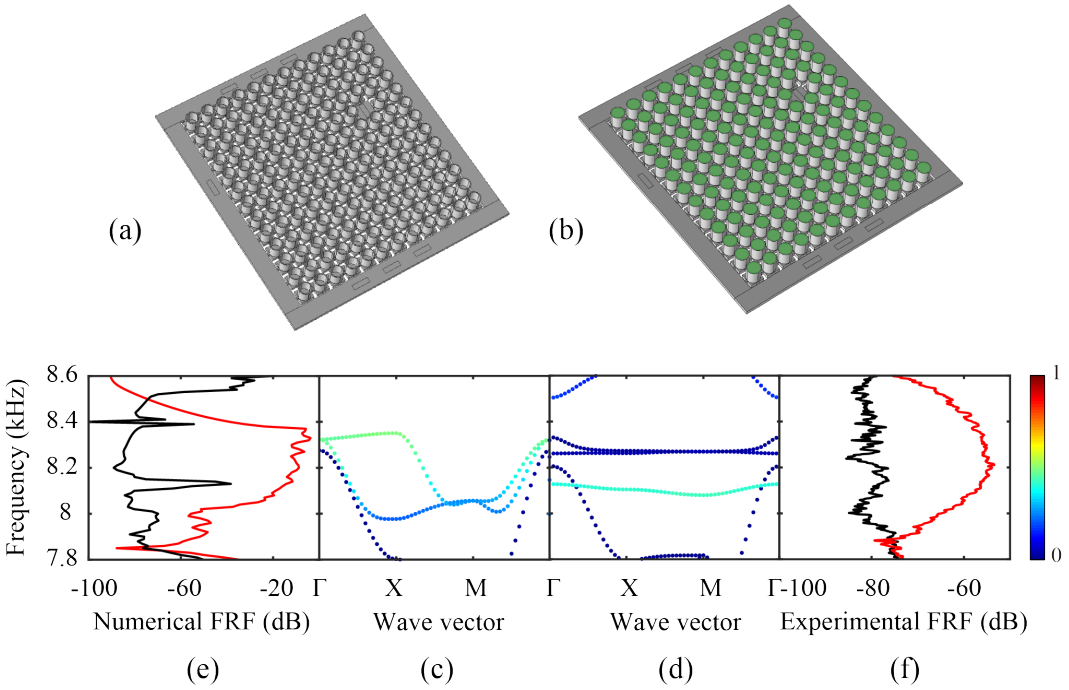

Figure 2: Schematic of the perfect epoxy metaplate (a) with all cups empty and (b) with all cups filled with water. The green and gray parts mark water and epoxy materials, respectively. The phononic band structure of the perfect epoxy metaplate without (c) and with (d) water filling the cups for a selected frequency range. The color scale measures the polarization amount of the out-of-plane component of displacement. Frequency response functions (FRFs) for the perfect phononic metaplate with all cups empty (red line) and filled with water (black line) obtained from simulation (e) and experiment (f) for a selected frequency range.

comparison. The properties of the bare phononic crystal can be considered with all cups either empty or filled with water, as depicted in Figs. 2(a,b). The phononic band structures of the infinite PC are different for empty or filled cups, as Figs. 2(c,d) show. Band structures are shown only within the frequency range of interest extending from 7.8 kHz to 8.6 kHz. Dispersion bands are classified as in-plane or out-of-plane by observing the polarization of the displacement vector for each Bloch wave. The color bar indicates the amount of vertical component in the displacement vector. Dark blue bands are disregarded, as their polarization is purely in-plane. Recently [45], we have have shown that transmission is strongly affected by the presence or absence of water inside the cups. This phenomenon was explained based on the local-resonance mechanism and the influence of the fluid-solid boundary condition [44]. With filled cups, there is only one flat band with out-of-plane polarization in the frequency region of interest, around 8.1 kHz; this flat band leads to some transmission in the numerical simulation but is hardly detected in the experiment. Conversely, with empty cups, passing out-of-plane bands appear and lead to partial transmission from 7.98 kHz to 8.35 kHz in the numerical simulation. Experimentally, partial transmission over an even wider bandwidth is observed. As a result, negative contrast can be used to define resonating defects in the phononic metaplate, i.e. by emptying given cups in the array of initially filled cups [45].

The numerical and experimental FRFs are fairly consistent without any parametric adjustment, as a comparison of Fig. 2(e) and Fig. 2(f) shows. In detail, the experimental FRFs appear to be shifted in frequency and have a wider frequency extension compared to the numerical results. The slight frequency shifts may be attributed to the difference of machining and material properties or the underestimated acoustoelastic coupling in the numerical simulation. Generally, the complete band gap for filled cups is suitable for the design of highly confined coupled resonator waveguides, as we discuss next. In the following, we investigate wave propagation in either periodic or aperiodic coupled-resonator acoustoelastic waveguides (CRAEWs) defined by negative contrast (defects are empty cups). It is expected that elastic waves can be spatially localized around the defects at the frequencies inside the complete band gaps, decaying

exponentially away from the defect center [8, 51, 32].

3. Results and discussion

We now consider CRAEWs formed in the perfect PC metaplate by locally emptying certain cups. We first consider a straight line of defects, with adjacent cavities separated by two lattice constants, as shown in Fig. 3(a). Figs. 3(b-d) present the phononic band structure of the CRAEW, as well as the numerical and experimental frequency response functions for the finite sample. The CRAEW supercell is shown in Fig. 3(e) together with a representative modal shape for the guided wave at point N_L. Looking closer at the band structure in Fig. 3(b), there are additional guiding bands that appear throughout the frequency range between 8.09 kHz to 8.27 kHz which is extremely sensitive to local changes in the resonators. In other words, its dispersion relationship is ultimately determined by the coupling strength between the resonators. The simulated and experimental frequency response functions in Figs. 3(c,d) indicate that transmission through the waveguide is indeed obtained. As in the case of the perfect crystals, the FRFs agree fairly well. It is noticed that there are 10 dB differences between the numerical simulations and the experiments in the FRF. This can possibly be attributed to the slightly inaccurate modeling of the sample, inaccurate material properties, evaporation of water during experiments, and the neglection of certain aspects of acoustoelastic coupling. On the other hand, the excitation sources of the simulations and experiments are not exactly the same. The vibrations for the eigenmode in Fig. 3(e) are mainly concentrated on the defect. There is some energy leakage to the adjacent unit cells ensuring coupling between subsequent defects. The eigenmode is also symmetric with respect to the direction of wave propagation. The out-of-plane displacement field for the finite sample is shown (f) for numerical simulation at 8.27 kHz and (g) for experiment at 8.16 kHz. Movies of the propagation of the guided waves are further shown in the Supplementary Material [52]. Propagation along the straight CRAEW is observed neatly. After the first row of the crystal, elastic energy is well confined in the defects along the waveguide.

Wave confinement along straight linear waveguides was discussed quantitatively before [45] and is here extended to the CRAEW case. A confinement degree [53] was proposed as follows:

$$C_x = \left(\frac{1}{l_y} \int \frac{1}{l_x} \int \left[\frac{|u_z|}{|u_z|_{max}} |x|^2 \right] \mathrm{d}x\mathrm{d}y \right)^{-1} \qquad (4)$$

where l_x and l_y are the lengths for one row of the finite structure in the x and the y directions. $|x|$ is the distance to the excitation source. The confinement degree calculated for the straight CRAEW is $C_x = 32.64\ \mathrm{m}^{-2}$, which implies a stronger confinement than inside the linear straight waveguide in the same phononic metaplate [45].

Next, we consider a bent CRAEW including a sharp corner with a 90° bend. Fig. 4(a) shows a schematic representation of the negative contrast bent CRAEW. In this case, the phononic band structure cannot be obtained. Instead, we can still obtain the frequency response function and compare it to the experimental result. The numerical (b) and experimental (c) FRFs are not significantly different from the straight CRAEW case. In particular, the transmission bandwidth are similar. The out-of-plane displacement field for the finite sample is shown (d) for numerical simulation at 8.12 kHz and (e) for experiment at 8.16 kHz. Movies of the propagation of the guided waves are further shown in the Supplementary Material [52]. Vibrations are again mainly confined at the defect sites where the cups are empty along the circuits. When looking closer to the displacement distributions, vibrations are similarly symmetric with respect to the direction of wave propagation before the bend, as for the straight CRAEW. Then symmetry with respect to the direction of propagation is broken. Vibrations are found to be a superposition of two orthogonal dipolar components, oriented along the x and the y axes, effectively inducing an elliptical vibration [45]. This effect can especially be observed in the animations shown in Supplementary Material [52]. A good consistency is perceived between numerical and experimental results. In addition, different from topological waveguides [48], the energy in bent CRAEW will be either reflected by the corner or confined by the periodicity. Obtaining a frequency-dependent number, such as a coefficient of transmission, indeed appears difficult.

As we know, evanescent coupling of waves across a band gap is omnidirectional, decreasing exponentially away from a resonator, that is why the coupling between adjacent resonators is not limited to the privileged crystallographic directions [46]. Therefore, evanescent waves suitably couple adjacent resonators placed along a rather arbitrary path, forming an aperiodic coupled-resonator chain [54, 55]. The collective resonances of a chain of coupled phononic microresonators have been achieved in the pure silica phononic structure in our previous work [46] where the defects are designed by omitting the etching of selected holes in a solid plate. Here, a similar chain of coupled acoustoelastic resonators, or an

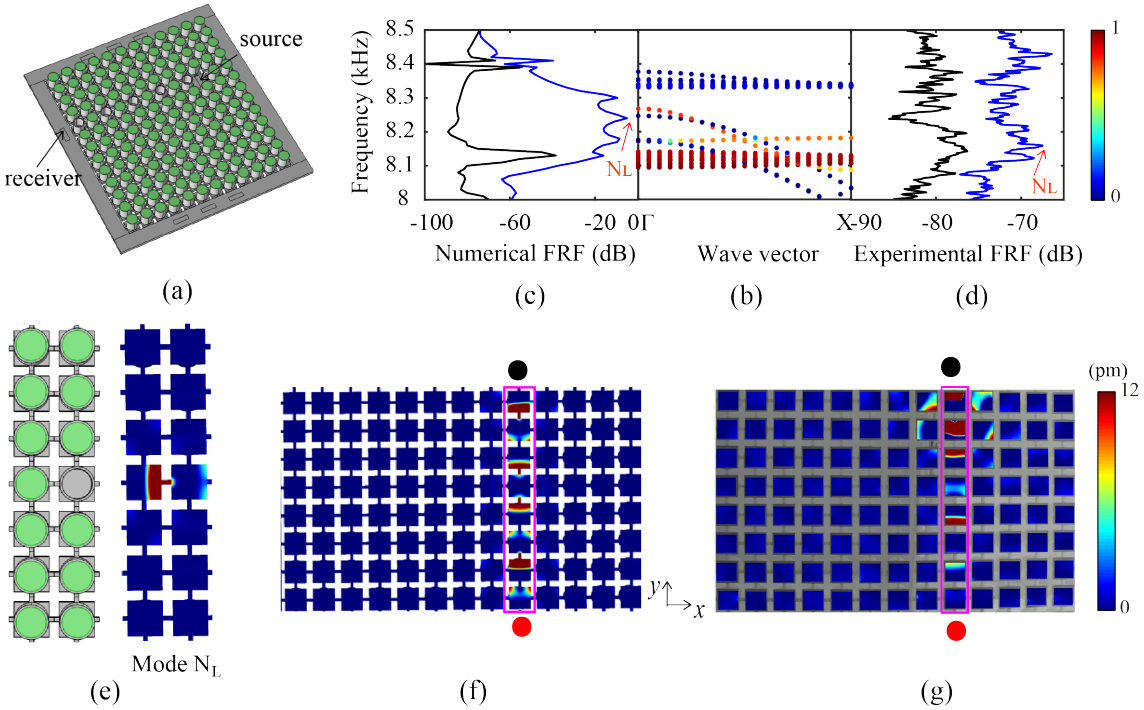

Figure 3: Schematic of the epoxy metaplate with a negative contrast straight CRAEW formed by locally emptying a line of cups (a). The green and gray parts mark water and epoxy materials, respectively. The phononic band structure (b) of perfect phononic metaplate with all cups filled with water (solid lines) the straight CRAEW (dash lines) for a selected frequency range. The frequency response functions (FRFs) of the perfect phononic metaplate with all cups filled with water (black line) and for the straight CRAEW (blue line) obtained from simulation (c) and experiment (d) for a selected frequency range. The CRAEW supercell and eigenmode N_L at the marked dispersion point are depicted in (e). The numerical (f) and experimental (g) out-of-plane displacement distributions are shown at 8.27 kHz and 8.16 kHz, respectively. The propagating circuits are surrounded by the pink lines. The black (red) disks indicate the wave source (receiver) positions. The color scales represent the amplitude of the out-of-plane displacement field from 0 (blue) to maximum (red).

aperiodic CRAEW, is designed by locally emptying certain cups separated by $(\pm 2, \pm 1)$ or $(\pm 1, \pm 2)$ lattice shifts, as shown in Fig. 5(a).

The numerical (b) and experimental (c) FRFs are presented in Fig. 5. A series of sharp resonances are clearly observed inside the initial complete band gap. As argued in Ref. [46], it can be explained from the discrete sequence of eigenfrequencies of the chain modeled as a phononic polymer. The maximum amplitude of the out-of-plane displacement for each peak varies notably, indicating that vibration modes are variously matched to the excitation source. The out-of-plane displacement field for the finite sample is shown in Fig. 5(d) for numerical simulation at 8.12 kHz and in Fig. 5(e) for experiment at 8.16 kHz. Movies of the collective vibrations are further shown in the Supplementary Material [52]. Clearly, the full chain of defects vibrates coherently. It can be noticed that the vibrations of the defect resonators along the chain are elliptical, in correspondence with the vibrations in the bent CRAEW after the bend. This effect results from the lack of periodicity of the chain and of the absence of symmetry with respect to the direction of propagation. Overall, guided waves are rather well confined inside the defect chain.

In the following, a simplified periodic version of the aperiodic CRAEW is considered to compare to some extent with the discrete structure. The supercell is depicted in Fig. 6(a). The sequence of lattice translations is $(2, -1)a$ then $(2, +1)a$ so that the spatial period along axis x is $4a$. The periodic CRAEW thus defined can be obtained from a continuous deformation of the chain of resonators. The phononic band structure for the supercell is shown in Fig. 6(b). A number of additional bands appear inside the complete band gap, as in the case of Fig. 3(b). These bands have different polarization contents and couple differently with the source of vibrations. As a remark, since two periods of the chain are actually included in the supercell compared to the periodic straight CRAEW as shown in Fig. 3, the $4a$ period causes spurious foldings at the Brillouin zone edges. As a result, the additional bands around 8.18 kHz extend almost asymmetrically and continuously toward the Γ and

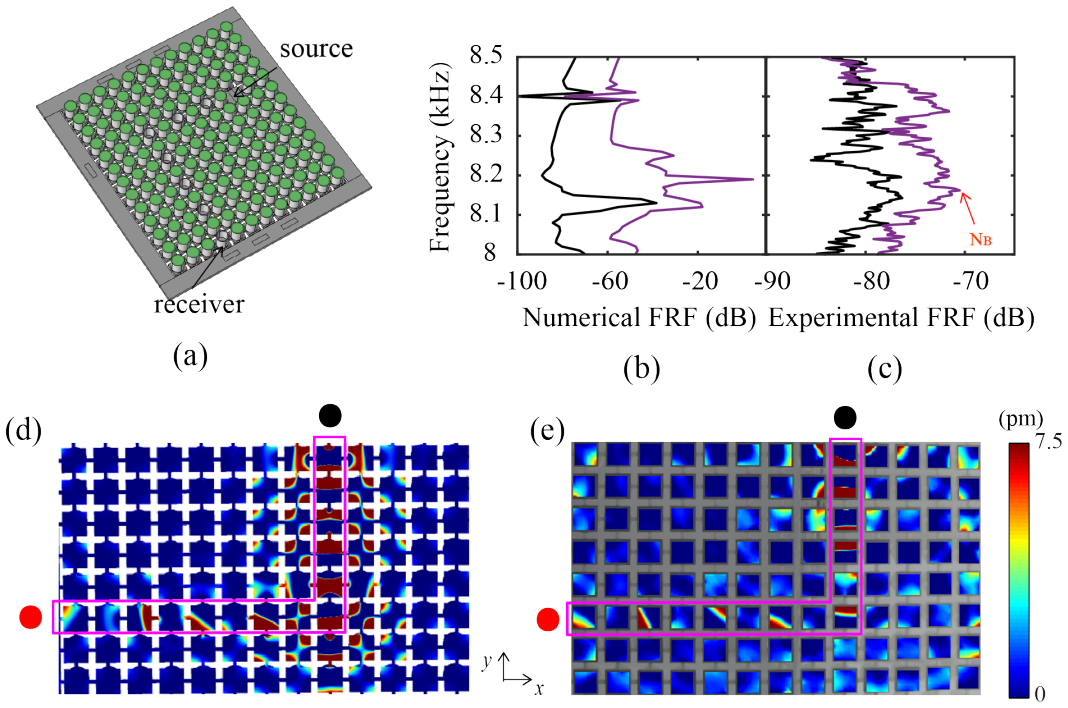

Figure 4: Schematic of the epoxy metaplate with a negative contrast bent CRAEW formed by locally emptying a bent line of cups (a). The green and gray parts mark water and epoxy materials, respectively. The frequency response functions (FRFs) of the perfect phononic metaplate with all cups filled with water (black line) and for the bent CRAEW (purple line) obtained from simulation (b) and experiment (c) for a selected frequency range. The out-of-plane displacement distributions at 8.12 kHz in the simulation (d) and 8.16 kHz in the experiment (e). The propagating circuits are surrounded by the pink lines. The black (red) disks indicate the wave source (receiver) positions. The color scale represents the amplitude of the out-of-plane displacement field from 0 (blue) to maximum (red).

X points, in contrast to the cosine shape of the bands of the straight CRAEW in Fig. 3(b). Therefore, coupling coefficients are almost independent of the direction of coupling. Figs. 6(c,d) also illustrate the eigenmodes at the high-symmetry points of the Brillouin zone around 8.18 kHz corresponding to points A and B. The elliptical vibration directions of both defect resonators are reversed at the Γ and X points. More significantly, the eigenmode shapes are clearly very similar to those observed in the collective vibrations of Fig. 6.

4. Conclusions

In this paper, wave propagation in coupled-resonator acoustoelastic waveguides formed by evanescent coupling of chains of defect cavities has been studied numerically and experimentally. Straight and bent periodic waveguides, and aperiodic circuits which are formed by locally emptying certain cups have been investigated. Localized defect modes existing inside the complete band gap are the basis of the wave guidance in CRAEWs and lead to strong wave confinement in the defects. Experimental results are found to be in fair agreement with numerical results in all cases. This work provides the first numerical and experimental realization of two-dimensional reconfigurable coupled-resonator acoustoelastic waveguides. Furthermore, to our knowledge it is the first time that acoustoelastic wave propagation along aperiodic CRAEWs is achieved, resulting in a larger choice for the definition of phononic circuits. This work provides prospects for the reconfigurable manipulation of acoustoelastic wave transmission in coupled-resonator waveguides. Different chains of CRAEWs with a rather arbitrary shape can indeed be straightforwardly realized without changing the solid metaplate. Active or even smart manipulation of localized resonators is thus expected.

Acknowledgments

The authors acknowledge financial support by the National Natural Science Foundation of China (12102350, 12122207, and 12021002). YW acknowledges support by the Natural Science Foundation of

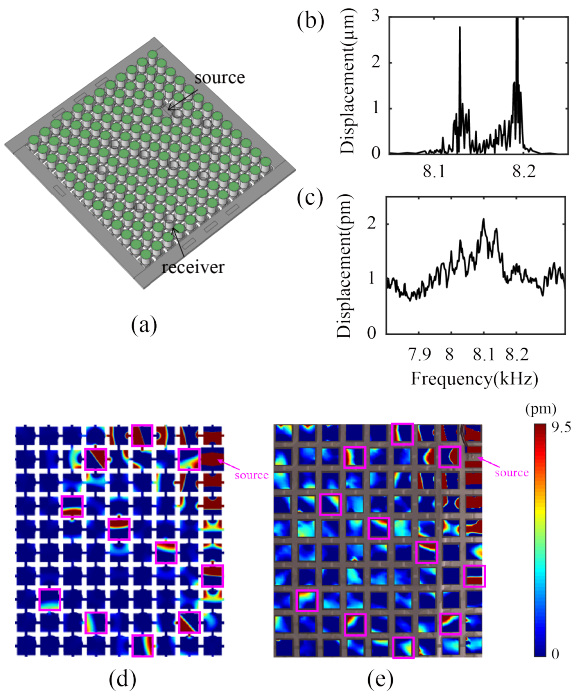

Figure 5: Schematic of the epoxy metaplate with a negative contrast aperiodic CRAEW of 11 coupled resonators formed by locally emptying a chain of cups (a). The absolute vertical displacements obtained from simulation (b) and experiment (c) at the position of the last resonator in the chain around selected frequencies. Vertical-displacement maps at frequencies of 8.18 kHz in the numerical simulation (d) and 8.19 kHz in the experiment (e). All the defect resonators along the chain are figured by the pink square. The color scale represents the amplitude of the out-of-plane displacement field from 0 (blue) to maximum (red).

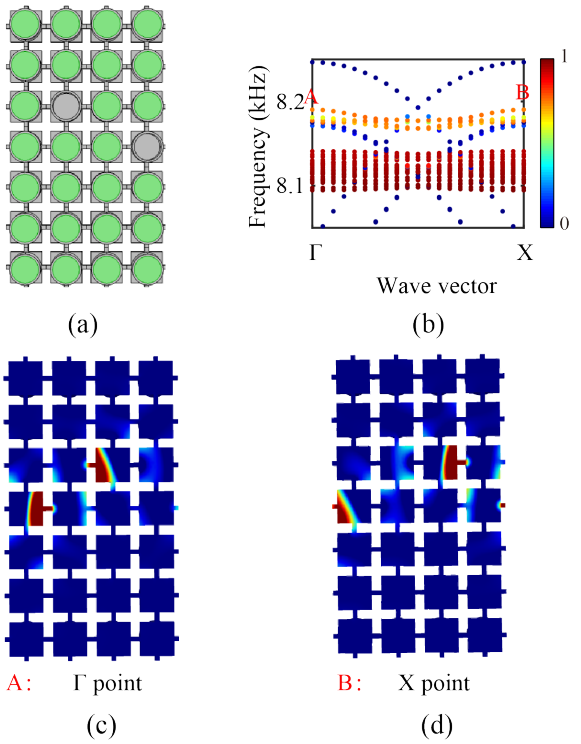

Figure 6: The supercell of calculation domain (a) and band structure (b) for aperiodic CRAEW. Eigenmodes of the supercell shown at the Γ point (c) and X point (d) of the first Brillouin zone at the passing band at 8.18 Hz. The color scale represents the amplitude of the out-of-plane displacement field from 0 (blue) to maximum (red).

Tianjin (20JCQNJC01030). V.L. acknowledges financial support by the EIPHI Graduate School (ANR-17-EURE-0002).

References

[1] E. Yablonovitch, Inhibited spontaneous emission in solid-state physics and electronics, Physical review letters 58 (1987) 2059.

[2] M. S. Kushwaha, P. Halevi, L. Dobrzynski, B. Djafari-Rouhani, Acoustic band structure of periodic elastic composites, Physical review letters 71 (1993) 2022.

[3] M. Sigalas, E. N. Economou, Band structure of elastic waves in two dimensional systems, Solid state communications 86 (1993) 141–143.

[4] V. Laude, Y. Achaoui, S. Benchabane, A. Khelif, Evanescent Bloch waves and the complex band structure of phononic crystals, Phys. Rev. B 80 (2009) 092301.

[5] J. S. Jensen, Phononic band gaps and vibrations in one-and two-dimensional mass–spring structures, Journal of Sound and Vibration 266 (2003) 1053–1078.

[6] X. An, H. Fan, C. Zhang, Elastic wave and vibration bandgaps in two-dimensional acoustic metamaterials with resonators and disorders, Wave Motion 80 (2018) 69–81.

[7] T.-T. Wang, Y.-F. Wang, Y.-S. Wang, V. Laude, Evanescent-wave tuning of a locally resonant sonic crystal, Applied Physics Letters 113 (2018) 231901.

[8] M. Torres, F. M. De Espinosa, D. Garcia-Pablos, N. Garcia, Sonic band gaps in finite elastic media: surface states and localization phenomena in linear and point defects, Physical Review Letters 82 (1999) 3054.

[9] Y. Pennec, J. O. Vasseur, B. Djafari-Rouhani, L. Dobrzyński, P. A. Deymier, Two-dimensional phononic crystals: Examples and applications, Surface Science Reports 65 (2010) 229–291.

[10] Y. Akahane, M. Mochizuki, T. Asano, Y. Tanaka, S. Noda, Design of a channel drop filter by using a donor-type cavity with high-quality factor in a two-dimensional photonic crystal slab, Applied Physics Letters 82 (2003) 1341–1343.

[11] R. Anufriev, M. Nomura, Heat conduction engineering in pillar-based phononic crystals, Physical Review B 95 (2017) 155432.

[12] M. Ghasemi Baboly, A. Raza, J. Brady, C. Reinke, Z. C. Leseman, I. El-Kady, Demonstration of acoustic waveguiding and tight bending in phononic crystals, Applied Physics Letters 109 (2016) 183504.

[13] P. H. Otsuka, K. Nanri, O. Matsuda, M. Tomoda, D. Profunser, I. Veres, S. Danworaphong, A. Khelif, S. Benchabane, V. Laude, et al., Broadband evolution of phononic-crystal-waveguide eigenstates in real-and k-spaces, Scientific reports 3 (2013) 1–5.

[14] M. Ghasemi Baboly, C. M. Reinke, B. A. Griffin, I. El-Kady, Z. Leseman, Acoustic waveguiding in a silicon carbide phononic crystals at microwave frequencies, Applied Physics Letters 112 (2018) 103504.

[15] Y. Pennec, B. Djafari-Rouhani, J. Vasseur, A. Khelif, P. A. Deymier, Tunable filtering and demultiplexing in phononic crystals with hollow cylinders, Physical Review E 69 (2004) 046608.

[16] Y. Jin, Y. Pennec, Y. Pan, B. Djafari-Rouhani, Phononic crystal plate with hollow pillars actively controlled by fluid filling, Crystals 6 (2016) 64.

[17] M. R. Singh, J. Guo, J. M. Cid, P. C. Sharma, A. H. Aly, B. Bhadoria, J. E. De Hoyos Martinez, Phonon conductivity of nanoparticles embedded in dielectric material, Physica Status Solidi (b) 255 (2018) 1700681.

[18] A. H. Aly, S. M. Shaban, A. Mehaney, High-performance phoxonic cavity designs for enhanced acousto-optical interaction, Applied Optics 60 (2021) 3224–3231.

[19] A. Rostami, H. Kaatuzian, B. Rostami-Dogolsara, Acoustic 1× 2 demultiplexer based on fluid-fluid phononic crystal ring resonators, Journal of Molecular Liquids 308 (2020) 113144.

[20] A. Nagaty, A. Mehaney, A. H. Aly, Acoustic wave sensor based on piezomagnetic phononic crystal, Journal of Superconductivity and Novel Magnetism 31 (2018) 4173–4177.

[21] S. M. Shaban, A. Mehaney, A. H. Aly, Determination of 1-propanol, ethanol, and methanol concentrations in water based on a one-dimensional phoxonic crystal sensor, Applied Optics 59 (2020) 3878–3885.

[22] A. H. Aly, A. Nagaty, A. Mehaney, One-dimensional phononic crystals that incorporate a defective piezoelectric/piezomagnetic as a new sensor, The European Physical Journal B 91 (2018) 1–5.

[23] S. E. Zaki, A. Mehaney, H. M. Hassanein, A. H. Aly, High-performance liquid sensor based one-dimensional phononic crystal with demultiplexing capability, Materials Today Communications 26 (2021) 102045.

[24] S. E. Zaki, A. Mehaney, H. M. Hassanein, A. H. Aly, Fano resonance based defected 1D phononic crystal for highly sensitive gas sensing applications, Scientific Reports 10 (2020) 1–16.

[25] H. Zhu, F. Semperlotti, Metamaterial based embedded acoustic filters for structural applications, AIP Advances 3 (2013) 092121.

[26] Y.-F. Wang, T.-T. Wang, J.-P. Liu, Y.-S. Wang, V. Laude, Guiding and splitting Lamb waves in coupled-resonator elastic waveguides, Composite Structures 206 (2018) 588–593.

[27] P. A. Deymier, Acoustic metamaterials and phononic crystals, volume 173, Springer Science & Business Media, 2013.

[28] A. Yariv, Y. Xu, R. K. Lee, A. Scherer, Coupled-resonator optical waveguide:? a proposal and analysis, Optics letters 24 (1999) 711–713.

[29] M. Notomi, E. Kuramochi, T. Tanabe, Large-scale arrays of ultrahigh-Q coupled nanocavities, Nature photonics 2 (2008) 741–747.

[30] R. Sainidou, N. Stefanou, A. Modinos, Linear chain of weakly coupled defects in a three-dimensional phononic crystal: A model acoustic waveguide, Physical Review B 74 (2006) 172302.

[31] J. M. Escalante, A. Martínez, V. Laude, Dispersion relation of coupled-resonator acoustic waveguides formed by defect cavities in a phononic crystal, Journal of Physics D: Applied Physics 46 (2013) 475301.

[32] A. Khelif, A. Choujaa, B. Djafari-Rouhani, M. Wilm, S. Ballandras, V. Laude, Trapping and guiding of acoustic waves by defect modes in a full-band-gap ultrasonic crystal, physical Review B 68 (2003) 214301.

[33] T.-T. Wang, S. Bargiel, F. Lardet-Vieudrin, Y.-F. Wang, Y.-S. Wang, V. Laude, Phononic coupled-resonator waveguide microcavities, Applied Sciences 10 (2020) 6751.

[34] Y.-F. Wang, T.-T. Wang, Y.-S. Wang, V. Laude, Reconfigurable phononic-crystal circuits formed by coupled acoustoelastic resonators, Physical Review Applied 8 (2017) 014006.

[35] S. Mohammadi, A. Khelif, A. Adibi, VHF phononic band gap band pass filters using coupled resonator acoustic waveguides (craw), in: 2011 IEEE International Ultrasonics Symposium, IEEE, 2011, pp. 2158–2160.

[36] Z. Hou, F. Wu, Y. Liu, Phononic crystals containing piezoelectric material, Solid State Communications 130 (2004) 745–749.

[37] T.-T. Wu, Z.-C. Hsu, Z.-G. Huang, Band gaps and the electromechanical coupling coefficient of a surface acoustic wave in a two-dimensional piezoelectric phononic crystal, Physical Review B 71 (2005) 064303.

[38] V. Laude, M. Wilm, S. Benchabane, A. Khelif, Full band gap for surface acoustic waves in a piezoelectric phononic crystal, Physical Review E 71 (2005) 036607.

[39] G. Trainiti, M. Ruzzene, Non-reciprocal elastic wave propagation in spatiotemporal periodic structures, New Journal of Physics 18 (2016) 083047.

[40] G.-H. Li, Y.-Z. Wang, Y.-S. Wang, Active control on switchable waveguide of elastic wave metamaterials with the 3d printing technology, Scientific reports 9 (2019) 1–8.

[41] Y. Pennec, V. Laude, N. Papanikolaou, B. Djafari-Rouhani, M. Oudich, S. El Jallal, J. C. Beugnot, J. M. Escalante, A. Martínez, Modeling light-sound interaction in nanoscale cavities and waveguides, Nanophotonics 3 (2014) 413–440.

[42] A. Hu, X. Zhang, F. Wu, Y. Yao, C. Cheng, P. Huang, Temperature effects on the defect states in two-dimensional phononic crystals, Physics Letters A 378 (2014) 2239–2244.

[43] M. Mazzotti, I. Bartoli, M. Miniaci, Modeling bloch waves in prestressed phononic crystal plates, Frontiers in Materials 6 (2019) 74.

[44] T.-T. Wang, Y.-F. Wang, Y.-S. Wang, V. Laude, Tunable fluid-filled phononic metastrip, Applied Physics Letters 111 (2017) 041906.

[45] T.-T. Wang, Y.-F. Wang, Z.-C. Deng, V. Laude, Y.-S. Wang, Reconfigurable waveguides defined by selective fluid filling in two-dimensional phononic metaplates, Mechanical Systems and Signal Processing 165 (2022) 108392.

[46] T.-T. Wang, S. Bargiel, F. Lardet-Vieudrin, Y.-F. Wang, Y.-S. Wang, V. Laude, Collective resonances of a chain of coupled phononic microresonators, Physical Review Applied 13 (2020) 014022.

[47] Y.-F. Wang, Y.-S. Wang, Multiple wide complete bandgaps of two-dimensional phononic crystal slabs with cross-like holes, Journal of Sound and Vibration 332 (2013) 2019–2037.

[48] M. Miniaci, M. Mazzotti, M. Radzieński, N. Kherraz, P. Kudela, W. Ostachowicz, B. Morvan, F. Bosia, N. M. Pugno, Experimental observation of a large low-frequency band gap in a polymer waveguide, Frontiers in Materials 5 (2018) 8.

[49] Y.-F. Wang, S.-Y. Zhang, Y.-S. Wang, V. Laude, Hybridization of resonant modes and Bloch waves in acoustoelastic phononic crystals, Physical Review B 102 (2020) 144303.

[50] V. Laude, M. E. Korotyaeva, Stochastic excitation method for calculating the resolvent band structure of periodic media and waveguides, Physical Review B 97 (2018) 224110.

[51] I. Psarobas, N. Stefanou, A. Modinos, Phononic crystals with planar defects, Physical Review B 62 (2000) 5536.

[52] See Supplemental Material at [URL will be inserted by publisher] for the animation of the numerical (a) and experimental (b) z-component of the displacement distribution of the epoxy metaplate with positive and negative contrast waveguides.

[53] Y.-F. Wang, Y.-S. Wang, C. Zhang, Bandgaps and directional propagation of elastic waves in 2D square zigzag lattice structures, Journal of Physics D: Applied Physics 47 (2014) 485102.

[54] S. Benchabane, R. Salut, O. Gaiffe, V. Soumann, M. Addouche,

V. Laude, A. Khelif, Surface-wave coupling to single phononic subwavelength resonators, Physical Review Applied 8 (2017) 034016.

[55] L. Raguin, O. Gaiffe, R. Salut, J.-M. Cote, V. Soumann, V. Laude, A. Khelif, S. Benchabane, Dipole states and coherent interaction in surface-acoustic-wave coupled phononic resonators, Nature communications 10 (2019) 1–8.